Two-photon interference of multimode two-photon pairs with an unbalanced interferometer

Hayato Goto, Haibo Wang, Tomoyuki Horikiri, Yasuo Yanagihara, and Takayoshi Kobayashi
Core Research for Evolutional Science and Technology (CREST), Japan Science and Technology Corporation (JST) and Department of Physics, Graduate School of Science, University of Tokyo, 7-3-1 Hongo, Bunkyo, Tokyo, 113-0033, Japan
(Received 10 July 2003; published 3 March 2004)

Two-photon interference of multimode two-photon pairs produced by an optical parametric oscillator has been observed with an unbalanced interferometer. The time correlation between the multimode two photons has a multipeaked structure. This property of the multimode two-photon state induces two-photon interference depending on the delay time.

DOI: 10.1103/PhysRevA.69.035801 PACS number(s): 42.50.St, 42.50.Ar, 42.65.Lm

Quantum interference is one of the most interesting phenomena in quantum physics. Since the observation of nonclassical effects in the interference of two photons by Ghosh and Mandel [1], several types of quantum interference experiments have been demonstrated using correlated two-photon pairs generated by spontaneous parametric downconversion (SPDC) [2–9]. In Refs. [1–9], higher visibility of two-photon interference than in the classical case is discussed as a typical nonclassical effect. Another feature of quantum interference is characterized by the shorter period of interference than in the classical case. Fonseca *et al.* have observed a twice narrower interference pattern than single-photon interference with correlated two-photon pairs generated by SPDC [10]. Quantum lithography has been proposed by Boto *et al.* in order to surpass the classical diffraction limit utilizing this feature of quantum interference [11]. D'Angelo *et al.* have reported a proof-of-principle quantum lithography [12]. This feature of quantum interference has also been confirmed using a conventional Mach-Zehnder interferometer [13].

In these quantum interference experiments, the SPDC process has been used to prepare correlated two photons. Ou and Lu have succeeded in generating correlated two photons which have a narrow bandwidth and a long correlation time ($\sim$10 ns) by using an optical parametric oscillator (OPO) [14,15]. This property of the two photons produced by an OPO has enabled us to directly observe their correlation function by coincidence counting. These narrow-band two-photon states have been used to observe nonclassical photon statistics [16]. Goto *et al.* have recently reported the observation of another type of correlated two photons—that is, multimode two photons produced by an OPO [17]. The correlation function of the multimode two-photon state has a multipeaked structure. In this Brief Report, we report an observation of two-photon interference of multimode two-photon pairs with an unbalanced interferometer. The block diagram of this experiment is shown in Fig. 1. The output beam from an OPO is incident at one of the input ports of an unbalanced interferometer. The correlation function of one of the outputs of the interferometer is observed with two photodetectors and a coincidence counter. First, we discuss briefly what happens in this experiment. Next, we explain our experimental setup and show our experimental results. Finally, we discuss our results with theoretical calculation of the correlation function of the output of the interferometer.

The distance between multimode two photons produced by an OPO is $n\tau_r c$, where τ_r is the round-trip time of the OPO cavity, c is the vacuum light speed, and n is an integer [17]. We assume that the propagation time difference T between the short and long paths in the interferometer is nearly equal to $\tau_r/2$. There are two cases, case 1 and case 2: in case 1, both photons are reflected or transmitted at the first beam splitter of the interferometer; in case 2, one of the two photons is reflected and the other is transmitted there. The distances between two photons in the output of the interferometer in case 1 and case 2 are $n\tau_r c$ and $(n+1/2)\tau_r c$, respectively. Therefore, the two-photon pairs in case 1 and case 2 will induce the peaks of coincidence counts at delay times $n\tau_r$ and $(n+1/2)\tau_r$, respectively. This enables us to distinguish case 1 and case 2 through the delay time. The height of the peaks of coincidence counts at delay times $(n+1/2)\tau_r$ will be constant with respect to the path-length difference of the interferometer because two photons in case 2 do not interfere with each other. On the other hand, in case 1, the two-photon pairs will provide two-photon interference because we cannot tell which path a two-photon pair propagates on. Therefore, the height of the peaks of coincidence counts at delay times $n\tau_r$ will change with respect to the path-length difference of the interferometer. Thus, it is expected that two-photon interference depending on delay time will be observed in this experiment.

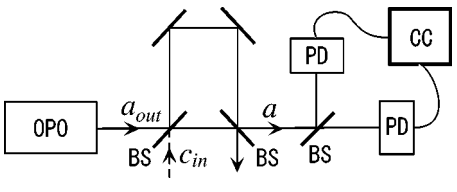

FIG. 1. Block diagram of the experiment. The output beam from an OPO is incident at one of the input ports of an unbalanced interferometer. The correlation function of one of the outputs of the interferometer is observed with two photodetectors and a coincidence counter. BS, 50-50 beam splitter; PD, photodetector; CC, coincidence counter.

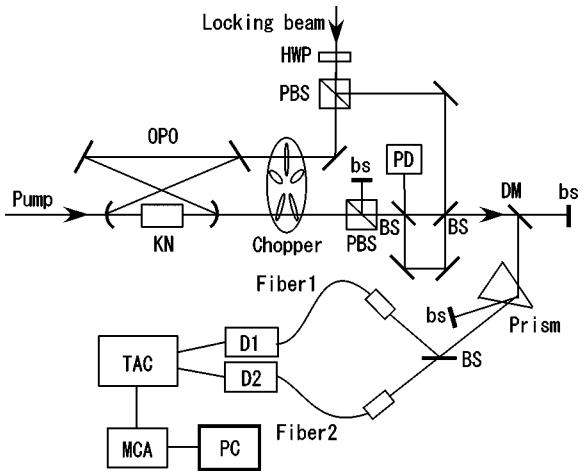

FIG. 2. Schematic of the experimental setup. PBS, polarization beam splitter; HWP, half-wave plate; PD, photodetector for phase lock; KN, $KNbO_3$ crystal; DM, dichroic mirror; BS, 50-50 beam splitter; bs, beam stop; D1 and D2, avalanche photodiodes; TAC, time-to-amplitude converter; MCA, multichannel analyzer.

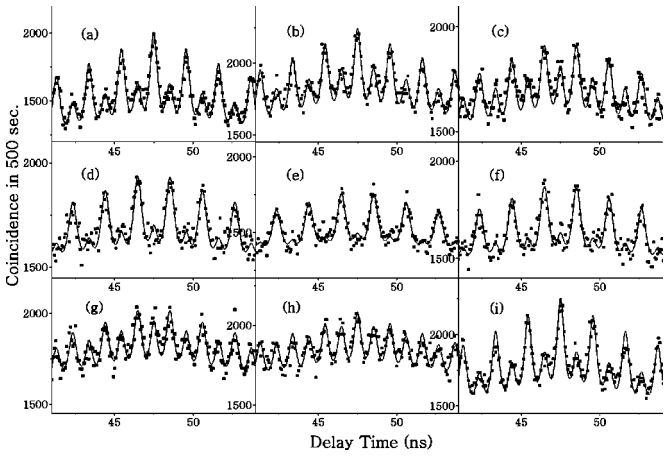

FIG. 3. Experimental results. The phase θ increases stepwise by $\pi/8$ from (a) to (i) [$\theta=(\pi/8)j,\ j=0,1,\ldots,8$]. The circles represent the measured coincidence counts. The lines are fits to Eq. (8), where fitting parameters are C_1, C_2, and θ. The fitting result of θ is shown in Fig. 4. The range of the data used for the fitting is from 18 ns to 77 ns.

The schematic of the experimental setup is shown in Fig. 2. The differences of this setup from that used in our previous work [17] are an unbalanced interferometer between the OPO and detectors and a locking beam for the phase lock of the interferometer. The light source is a single-mode cw Ti:sapphire laser of wavelength 860 nm. The round-trip length of the OPO is set long (560 mm) in order to time resolve the oscillatory structure in the correlation function. The output beam from the OPO is incident at one of the input ports of the interferometer. The path-length difference of the interferometer is set at about 29 cm, which gives $T \simeq 0.97$ ns. The phase difference of the interferometer is locked by a servo-control system. The locking beam for the interferometer propagates in the interferometer in the opposite direction to the signal beam from the OPO to avoid the locking beam to be detected by photodiodes. Furthermore, the polarization of the locking beam is perpendicular to that of the signal in order to remove the locking beam by a polarization beam splitter (see Fig. 2). One of the two outputs of the interferometer is split into two with a 50-50 beam splitter. The two beams are coupled to optical fibers and detected with avalanche photodiodes (APD's, EG&G SPCM-AQR-14). The coincidence counts of the signals from the two APD's are measured with a time-to-amplitude converter (TAC, ORTEC 567) and a multichannel analyzer (MCA, NAIG E-562). We measured the coincidence counts at $\theta=(\pi/8)j$ ($j=0,1,\ldots,8$), where θ is the phase difference of the interferometer defined as the intensity of the output of the interferometer is proportional to $(1+\cos\theta)$ when classical light of wavelength 860 nm is incident to the interferometer. The experimental results at $\theta=(\pi/8)j$ ($j=0,1,\ldots,8$) are shown in Figs. 3(a)–3(i).

In order to discuss our experimental results, we derive the correlation function of the output of the interferometer. The output operator $\tilde{a}(t)$ of one of the output ports of the interferometer is expressed as

$$\tilde{a}(t)=\frac{\tilde{a}_{out}(t-T_S)+\tilde{c}_{in}(t-T_S)}{2}-\frac{\tilde{c}_{in}(t-T_L)-\tilde{a}_{out}(t-T_L)}{2}. \tag{1}$$

Here $T=T_L-T_S$ is the propagation time difference between the short and long paths in the interferometer, and $\tilde{a}(t)$ denotes a Fourier transform of a field operator, $a(\Omega)$, of frequency $\omega_0+\Omega$ (ω_0 is the degenerate frequency of the OPO). That is, it is defined as

$$\tilde{a}(t)=\frac{1}{\sqrt{2\pi}}\int d\Omega a(\Omega)e^{-i(\omega_0+\Omega)t}. \tag{2}$$

a_{out} is the output operator of the OPO far below threshold [17] and c_{in} is an annihilation operator of the vacuum entering the interferometer from the other of the input ports (see Fig. 1). cT_S and cT_L are the short and long path lengths of the interferometer, respectively. The intensity correlation function is derived as follows [15,17]:

$$\begin{aligned}\Gamma(\tau)&=\langle\tilde{a}^{\dagger}(t)\tilde{a}^{\dagger}(t+\tau)\tilde{a}(t+\tau)\tilde{a}(t)\rangle\\&=\left[\frac{2\sqrt{\Gamma_0(\tau)}\cos\theta+\sqrt{\Gamma_0(\tau-T)}+\sqrt{\Gamma_0(\tau+T)}}{4}\right]^2\\&\quad+\left|\frac{2\sqrt{\delta\Gamma_0(0)}+e^{i\theta}\sqrt{\delta\Gamma_0(-T)}+e^{-i\theta}\sqrt{\delta\Gamma_0(T)}}{4}\right|^2\\&\quad+\left|\frac{2\sqrt{\delta\Gamma_0(\tau)}+e^{i\theta}\sqrt{\delta\Gamma_0(\tau-T)}+e^{-i\theta}\sqrt{\delta\Gamma_0(\tau+T)}}{4}\right|^2,\end{aligned} \tag{3}$$

with

$$\Gamma_0(\tau)=|\epsilon|^2\left(\frac{F}{F_0}\right)^2e^{-\Omega_c|\tau|}\frac{\sin^2[(2N+1)\Omega_F\tau/2]}{\sin^2(\Omega_F\tau/2)}, \tag{4}$$

$$\delta = \frac{4|\epsilon|^2}{\Omega_c^2}. \tag{5}$$

Here ϵ is the single-pass parametric amplitude gain; F and F_0 are the finesse of the OPO with and without loss, respectively; Ω_c and Ω_F are the bandwidth and free spectral range of the OPO, respectively; $2N+1$ is the number of the longitudinal modes in the OPO output. $\Gamma_0(\tau)$ is a multipeaked function of delay time τ. The width of the peaks is about $\tau_r/(2N+1)$. It is assumed that T is close to $\tau_r/2$ and the difference between them is longer than the width of the peaks. This assumption is well satisfied in our experiment. This allows the approximations

$$\Gamma_0(\tau)\Gamma_0(\tau \pm T) \simeq 0, \quad \Gamma_0(\tau - T)\Gamma_0(\tau + T) \simeq 0,$$
$$\Gamma_0(\pm T) \simeq 0. \tag{6}$$

In addition, δ is much smaller than one when the OPO is operated far below threshold. Therefore, Eq. (3) can be approximated as follows:

$$\Gamma(\tau) \simeq \frac{\Gamma_0(\tau)\cos^2\theta}{4} + \frac{\Gamma_0(\tau - T) + \Gamma_0(\tau + T)}{16} + \frac{\delta\Gamma_0(0)}{4}. \tag{7}$$

The first term on the right-hand side of Eq. (7) corresponds to two-photon interference in case 1. The second term on the right-hand side of Eq. (7), which is constant with respect to θ, corresponds to coincidence counts in case 2. These two terms are due to correlated two photons. The last term on the right-hand side of Eq. (7) corresponds to the contribution from higher photon-number states than 2. This term is not negligible when the pump intensity for the OPO is relatively high. As discussed in Ref. [17], the coincidence rate measured in experiments is an average of the correlation function over the resolving time T_R of detectors. According to Ref. [17], the coincidence counts measured in this experiment will become

$$\Gamma_c(\tau) = C_1[4\Gamma_c^{(0)}(\tau)\cos^2\theta + \Gamma_c^{(0)}(\tau - T) + \Gamma_c^{(0)}(\tau + T)] + C_2, \tag{8}$$

with

$$\Gamma_c^{(0)}(\tau) = e^{-\Omega_c|\tau - \tau_0|}\sum_n \left(1 + \frac{2|\tau - n\tau_r - \tau_0|\ln 2}{T_R}\right) \times \exp\left(-\frac{2|\tau - n\tau_r - \tau_0|\ln 2}{T_R}\right). \tag{9}$$

Here C_1 and C_2 are constants and τ_0 is an electric delay. The lines in Fig. 3 are fits to Eq. (8). The fitting parameters are two constants C_1 and C_2 and the phase difference θ. Constant parameters are set as follows: $\tau_0 = 47.5$ ns, $\tau_r = 2.07$ ns, $T_R = 280$ ns, and $\Omega_c/(2\pi) = 11$ MHz. The range of data used for the fitting is from 18 ns to 77 ns, while the range plotted in Fig. 3 is from 41 ns to 54 ns. The term C_2, independent of the delay time τ, is mainly due to the last term on the right-hand side of Eq. (7). In our experiment, C_2 is comparable to C_1. It means that the pump intensity for the OPO is relatively high and the contribution from higher photon-number states than 2 is not negligible. The phase determined from the fitting is plotted in Fig. 4 against the phase locked experimentally. The inclination of the line in Fig. 4 is unity. The error bars are estimated from the fluctuation of the phase. The deviations of the circles from the line are probably due to the fluctuation of the phase difference, which is shown by error bars in Fig. 4, and due to an imperfect visibility, which makes larger the deviations around $\theta = 0$, $\pi/2$, and π. Taking these points into consideration, Figs. 3 and 4 show a fairly good agreement between the experiment and theory.

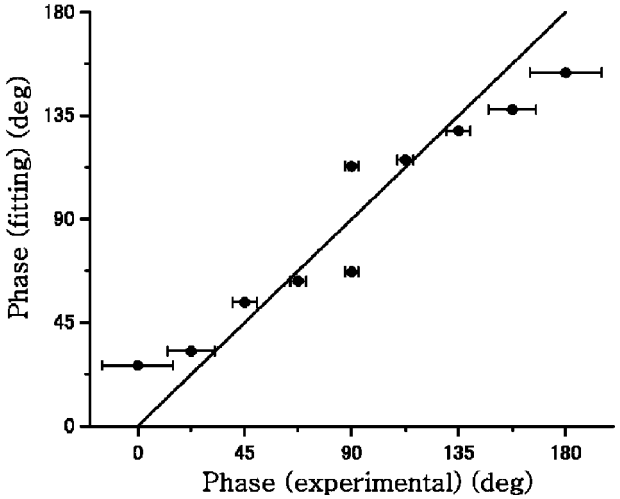

FIG. 4. Phase (fitting) determined by the fitting shown in Fig. 3 is plotted against phase (experimental), which is the phase locked experimentally. The inclination of the line is unity. The error bars are estimated from the fluctuation of the phase.

In conclusion, we have observed two-photon interference of multimode two-photon pairs produced by an OPO with an unbalanced interferometer. This two-photon interference is dependent on the delay time. The experimental results have been explained theoretically. In our experiment, the visibility of the two-photon interference was not high probably owing to the relatively high pump intensity for the OPO. Higher visibility will be observed with a lower-intensity pump.

[1] R. Ghosh and L. Mandel, Phys. Rev. Lett. **59**, 1903 (1987).
[2] C. K. Hong, Z. Y. Ou, and L. Mandel, Phys. Rev. Lett. **59**, 2044 (1987).
[3] Z. Y. Ou and L. Mandel, Phys. Rev. Lett. **62**, 2941 (1989).
[4] Z. Y. Ou, X. Y. Zou, L. J. Wang, and L. Mandel, Phys. Rev. A **42**, 2957 (1990).
[5] Z. Y. Ou, X. Y. Zou, L. J. Wang, and L. Mandel, Phys. Rev. Lett. **65**, 321 (1990).

[6] P. G. Kwiat, W. A. Vareka, C. K. Hong, H. Nathel, and R. Y. Chiao, Phys. Rev. A **41**, 2910 (1990).
[7] J. G. Rarity, P. R. Tapster, E. Jakeman, T. Larchuk, R. A. Campos, M. C. Teich, and B. E. A. Saleh, Phys. Rev. Lett. **65**, 1348 (1990).
[8] J. Brendel, E. Mohler, and W. Martienssen, Phys. Rev. Lett. **66**, 1142 (1991).
[9] Y. H. Shih, A. V. Sergienko, M. H. Rubin, T. E. Kiess, and C. O. Alley, Phys. Rev. A **49**, 4243 (1994).
[10] E. J. S. Fonseca, C. H. Monken, and S. Pádua, Phys. Rev. Lett. **82**, 2868 (1999).
[11] A. N. Boto, P. Kok, D. S. Abrams, S. L. Braunstein, C. P. Williams, and J. P. Dowling, Phys. Rev. Lett. **85**, 2733 (2000).
[12] M. D'Angelo, M. V. Chekhova, and Y. Shih, Phys. Rev. Lett. **87**, 013602 (2001).
[13] K. Edamatsu, R. Shimizu, and T. Itoh, Phys. Rev. Lett. **89**, 213601 (2002).
[14] Z. Y. Ou and Y. J. Lu, Phys. Rev. Lett. **83**, 2556 (1999).
[15] Y. J. Lu and Z. Y. Ou, Phys. Rev. A **62**, 033804 (2000).
[16] Y. J. Lu and Z. Y. Ou, Phys. Rev. Lett. **88**, 023601 (2002).
[17] H. Goto, Y. Yanagihara, H. Wang, T. Horikiri, and T. Kobayashi, Phys. Rev. A **68**, 015803 (2003).